BREAD CRUMB CLASSIFICATION USING FRACTAL AND MULTIFRACTAL FEATURES

Rodrigo Baravalle[a], **Claudio Delrieux**[b] **and Juan Carlos Gómez**[a]

[a]*Laboratorio de Sistemas Dinámicos y Procesamiento de Información, FCEIA, Universidad Nacional de Rosario, - CIFASIS - CONICET, Riobamba 250 bis, 2000, Rosario, Argentina, {baravalle,gomez}@cifasis-conicet.gov.ar, http://www.fceia.unr.edu.ar/lsd/*

[b]*DIEC, Universidad Nacional del Sur - IIIE-CONICET, Avenida Colón 80 - Bahía Blanca(8000FTN) - Provincia de Buenos Aires - República Argentina, cad@uns.edu.ar, http://www.ingelec.uns.edu.ar/*

Keywords: Fractal, Multifractal, Classification, Bread crumb, Support Vector Machines

Abstract. Adequate image descriptors are fundamental in image classification and object recognition. For this purpose, it is required to identify image features that are both robust and of low dimensionality, in a way such that the classification process can be performed in a variety of situations and with a reasonable computational cost.

In this context, the identification of materials posses a significant challenge, since usual (geometric and/or differential) feature extraction methods are not robust enough. Texture features based on Fourier or wavelet theories, on the other hand, do withstand geometric and illumination variations, but tend to require a high amount of descriptors to perform adequately.

Recently, the theory of fractal sets has shown to provide local image features that are both robust and low-dimensional. In this work we apply fractal and multifractal feature extraction for bread crumb classification based on color scans of slices of different bread types. Preliminary results show that fractal based classification is able distinguish different bread crumbs with very high accuracy.

1 INTRODUCTION

Fractal and multifractal analysis of images have demonstrated to capture useful properties of the underlying material represented. Characterisation of images using these features have been successfully applied in different fields, for instance medicine Andjelkovic et al. (2008); Yu and Qi (2011) and texture classification Wendt et al. (2009). Through several procedures, it is possible to obtain differents Fractal Dimensions (FD), each of them capturing a different property of the material (e.g., void fraction, rugosity).

For each material, the results obtained in the classification process are useful in quality measurements of real samples and also in the validation of synthetic representations of them. In other words, the classification is useful to determine if a given image presents the observed features in that material, permitting to establish quality parameters to them. In Fan and Zhang (2006), a quality bread crumb test was performed, obtaining good results. Nevertheless, a small database was used (30 images). In Gonzales-Barron and Butler (2008) several fractal features were obtained for one type of bread, showing that a vector comprising them would be capable of obtaining key features of its crumb texture.

In this work we propose the application of fractal and multifractal descriptors to classify among different bread types and to discriminate between bread and non-bread images. The proposed method is compared to a classifier that uses only mean color information. The results of this feature extraction procedure are shown to be both robust and simple to discriminate bread images from non bread ones. In section 2 we briefly introduce the theory underlying fractal sets. In section 3 we describe the materials and methods employed in the classification. In section 4 we show the results obtained in the classification and we perform a robustness analysis of the method. In section 5 we summarise the conclusions, and we pose some possible future works.

2 FEATURES

2.1 Box Dimension

Box FD is a simplification of the Hausdorff (originally Minkowski - Bouligand) dimension for non strictly self-similar objects Peitgen et al. (2004). Given a binarised image, it is subdivided in a grid of size $M \times M$ where the side of each box formed is ϵ. If N_ϵ represents the amount of boxes that contains at least one pixel in the binarisation of the set for that ϵ, then the computation of the box dimension D_b is as shown in Eq. (1).

$$D_b = \lim_{\epsilon \to 0} \frac{\log(N_\epsilon)}{\log(1/\epsilon)}. \tag{1}$$

The algorithm computes a binarised image of the original and then selects differents ϵ in it, making a count of the boxes that contains pixels in each case (to avoid numerical instabilities, a mean of cases is computed, establishing differents positions in the grid over the image). Finally, a linear regression adjustment is made with the obtained data, in the $\log - \log$ space, and the slope of the data is by definition the box dimension of the image. In Fig. 1 an image of the bread type *salvado* is shown with its box dimension computation.

2.2 Morphological Fractal

This FD is computed through dilation and erosion operations, using a structuring element (SE). The transformed image is function of the distribution of that particular SE in the original

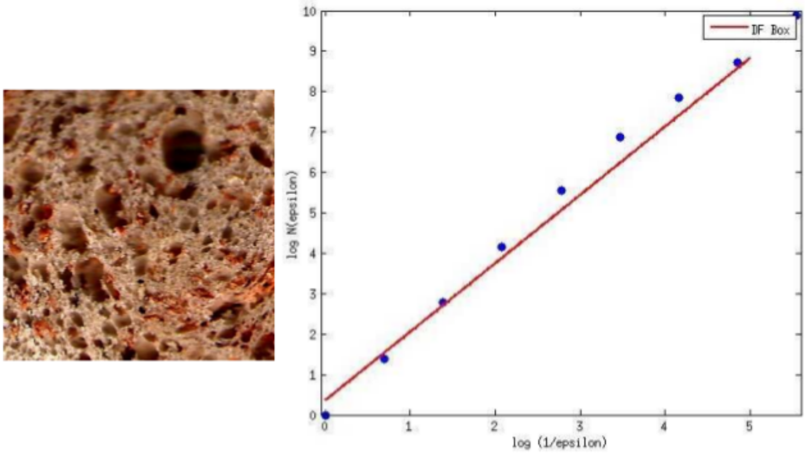

Figure 1: An image and its box dimension computed

image. In this case, the SE is a rhombus Y with scales that varies from $\epsilon = 1$ to $\epsilon = 7$ (and the areas of the SE between 5 and 113 pixels) . The surface area can be calculated, for each ϵ as in Eq. (2) Gonzales-Barron and Butler (2008).

$$S(X, Y, \epsilon) = \frac{\sum_{x,y \in M}(f^u_\epsilon(x, y) - f^l_\epsilon(x, y))}{2\epsilon}. \tag{2}$$

$f^u_\epsilon(x, y)$ is the ϵ-th dilation and $f^l_\epsilon(x, y)$ is the ϵ-th erosion of the original image. The morphological FD M_d is estimated from the slope of a linear regression adjustment of the data in $S(X, Y, \epsilon)$ and ϵ in the $\log - \log$ space.

$$M_d = 2 + m. \tag{3}$$

2.3 Multifractal Analysis

Some elements in nature show fractal features or auto similarity. The fractal dimension is an exponent which relates the statistical auto similarity of the object at different scales. On the one hand, deterministic fractals are characterized by the same FD at all scales. They are called *monofractals* (for instance, Koch Curve, Sierpinsky triangle). On the other hand, *multifractals* Mandelbrot (1989) are characterized by a set of FDs depending on the scale. It is assumed that these structures are composed by different fractals coexisting simultaneously. In a previous work Baravalle et al. (2012), it has been shown, using the Box Dimension and the Korcak Dimension Imre et al. (2011), that the bread crumb texture presented multifractal features. As a consequence, fractal and multifractal features are taken into account.

Hölder Exponent

Informally, the way to proceed with multifractal analysis is to examine, in the limit, the local behaviour of a measure μ at each point of the set in study. This means, to find the Hölder exponent α in that point. The *multifractal spectrum* $f(\alpha)$ is obtained applying this procedure to the entire set, in this case, an image.

Let E be an structure divided in substructures E_i of size ϵ in such a way that $U_i E_i = E$. Each substructure E_i is characterized by a measure $\mu(E_i)$. From the point of view of multifractal analysis, it is useful to define this value as a function of ϵ.

$$\alpha_i = \frac{ln(\mu(E_i))}{ln(\epsilon)}, \tag{4}$$

and to take the limit when ϵ tends to 0. The limit represents the value of the Hölder exponent at a point in the structure.

$$\alpha = \lim_{\epsilon \to 0} \alpha_i, \tag{5}$$

The exponent characterizes the local regularity of the structure at a point. To obtain a global characterization of its regularity it is needed to obtain the distribution of α in E. For this, a count must be done for each α_i, related to the value of ϵ (Eqn. 6).

$$f_\epsilon(\alpha_i) = -\frac{ln(N_\epsilon(\alpha_i))}{ln(\epsilon)}, \tag{6}$$

When ϵ tends to 0, the limiting value is the FD of the structure E characterized by α, the Hausdorff dimension of the α distribution, also known as the *multifractal spectrum* $f(\alpha)$ Silvetti and Delrieux (2010) (Eq. 7)

$$f(\alpha) = \lim_{\epsilon \to 0} f_\epsilon(\alpha). \tag{7}$$

Procedure

To obtain the Hölder exponent at a given pixel, a linear regression adjustment is needed using the values ($log(\epsilon)$,$log(\mu(E_i))$), for $\epsilon = 2i+1, i \geq 0$, where E_i are boxes of side ϵ centered at the pixel. The slope of the adjustment is the desired Hölder exponent.

From the α values a new image is generated in grey scale (α image), with the same dimensions of the original, where the value at each pixel is a mapping from the exponent to that scale. Since it is possible to obtain $M \times M$ values per image (where $M \times M$ is the dimension in pixels of the image), it is necessary to define a number C of classes (the number could be a parameter), each of which establish α range values, and calculate the spectrum only for those values.

Let α_{min} and α_{max} be the minimum and maximum values of α computed in the image. C values are defined $\alpha_c = \alpha_{min} + (c-1)(\alpha_{max} - \alpha_{min})/C$, where $c = 1, 2, \ldots, C$. Then, $\alpha \in \alpha_c$ if $\alpha_c \leq \alpha < \alpha_{c+1}$. If $\alpha = \alpha_{max}$, then $\alpha \in \alpha_C$. Finally, a linear regression adjustment is obtained for the values $N_\epsilon(\alpha)$ and ϵ in the $\log - \log$ space. The value of the slope is the FD $f(\alpha_c)$ and must be calculated for $c = 1, 2, \ldots, C$. In this way C $f(\alpha)$ values are obtained, representing C FDs (C α_c associated values are also obtained). In this work, all these values are used as features in the classification (so $2 \times C$ features are obtained from the multifractal analysis). In Fig. 2 an image of *lactal* bread type and its multifractal spectrum are shown (in this case, $C = 20$).

3 MATERIALS AND METHODOLOGY

3.1 Image Acquisition

UNIFY Fifty images of four different bread types (lactal, baguette, salvado and sandwich), counting two hundred (200) images, were obtained using an electric slicer. The images were digitalised

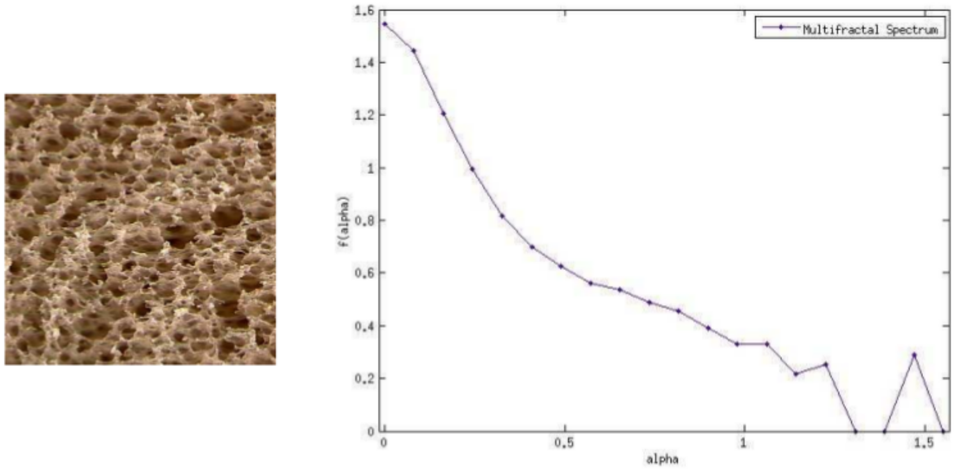

Figure 2: Image and its multifractal spectrum (20 FDs)

using an HP PSC 1210 scanner and they were saved in TIFF format. Images showed a resolution of 380×380 pixels (the maximum possible area for the four bread types) and 350 dpi (1 pixel - $0.00527 mm^2$). Then they were converted to grey scale (8 bits). Also 20 images of each bread type were taken with a digital camera, using the same spatial resolution, counting 80 images. The illumination conditions of these images were different from that of the scanner in order to test for the robustness of the method. In Fig. 5 four examples of bread images from the camera are shown. We also employed randomly 100 selected images from the CalTech101 Fei-Fei et al. (2004) dataset in order to test the method's performance with non-bread images. In Fig. 4 four examples of non-bread images from this dataset are shown. NORMALIZATION

For the FDs that uses a binarisation of the original image, the algorithm presented in White and Rohrer (1983) was utilised. This algorithm applies a local thresholding schema, which showed better results than using a global thresholding schema. Particularly, the algorithm presented in Huang and Wang (1995) and used in Gonzales-Barron and Butler (2008), showed poor results when the illumination conditions varies. Also an adjustment needs to be made since the center of air bubbles with bigger areas appeared as black pixels, instead of white (and since those areas are characterized as dark regions in the original image), a global grey threshold is obtained using Otsu's algorithm Otsu (1979). Then this threshold is multiplied with a scalar which is a parameter, defining as white the pixels with grey values below the threshold. It was found that defining the scalar as 0.8 showed acceptable results. So the combination of local and global thresholding makes it an hybrid algorithm. In Fig. 3 an image of each bread type used in this work and its resulting binarisation using the proposed algorithm is shown.

3.2 Feature Vectors

Following the ideas presented in Gonzales-Barron and Butler (2008), the mentioned fractal and multifractal features were obtained for each image (using 20 Hölder exponents). For each image, a 42 feature vector was computed. The code of the algorithms Box dimension, Morphological fractal dimension and the multifractal spectrum was written and run in Matlab. In order to make a comparison, a vector with RGB color features was computed (R mean, G mean, B mean) in a 3 dimension feature vector.

A self-organizing maps (SOM) Kohonen et al. (2001) of the vectorized images are useful

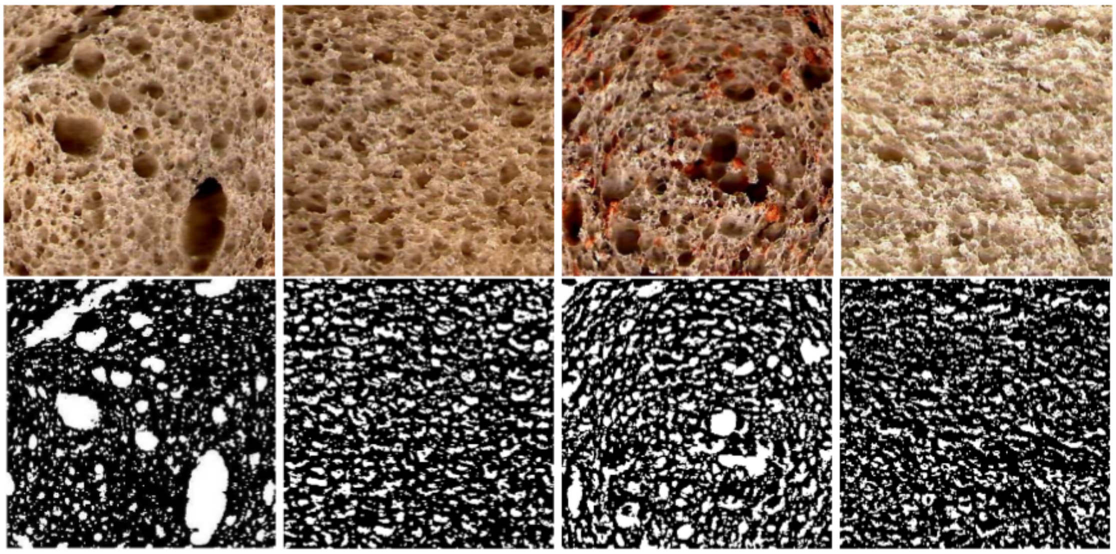

Figure 3: Digitalised images of Baguette, Lactal, Salvado and Sandwich bread types with its binarisations

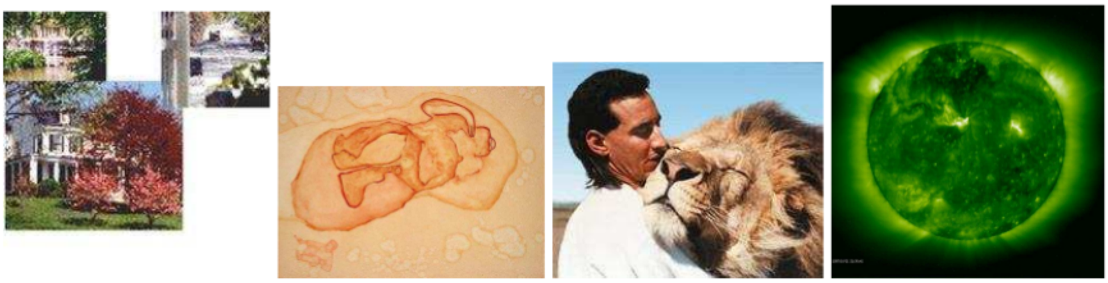

Figure 4: Images from the dataset CalTech101

to visualize these different representation of bread images into a lower dimensional view, in order to understand them better. A SOM maps high dimensional data into a (tipically) two-dimensional representation, using neighborhood information. Topological information of the original data is preserved.

An unsupervised SOM of the fractal and non fractal representation of scanned images are shown in Fig. 6a and Fig. 6b respectively. The fractal features SOM seems to show easily separable classes and the RGB features SOM appears to be more overlapped. Also, in the latter, the non bread class seems to be spread over the rest of the classes, making it more difficult to distinguish between bread and non bread types. It seems that a classificator could potentially obtain better classification results using the fractal features.

4 RESULTS

4.1 Classification

INTRODUCED BY

Support Vector Machines (SVM) Boser et al. (1992) were utilised to perform the classification, using *libsvm* Chang and Lin (2011) implementation. The method *k-fold cross validation* was utilised in order to validate the results with $k = 4$, i.e., 75% of samples are used as training and 25% as test (then switching the training and test samples). Table 1 shows classification results for both methods of classification, using 50 scanned images of each type (i.e. 250 images,

Figure 5: Digitalised images from a digital camera

including 50 of non bread images). It can be seen that the utilisation of non-fractal features in the images gives comparable results to that of using fractals features.

Features	Fractals	non Fractals
Accuracy	**88.4**%	86%

Table 1: Results obtained in classification

4.2 Robustness Test

In order to test for the robustness of the method, 20 scanned images from each class, and 20 from the CalTech101 dataset, were used as train and all the images from the digital camera (20 per class), and 20 non bread images were used as test (100 images for train and 100 images for test). In Table 2 accuracy results of both methods are shown. Results shows poor performance of both classifiers. In Tables 3 and 4, the confusion matrix of the data using both methods is shown. It can be seen that the RGB method assigns all the data to the non bread class, while the fractal features are able to discriminate between images of breads and non breads, making it a good discriminator of non bread images.

Features	Fractals	non Fractals
Accuracy	**40**%	20%

Table 2: Results for the robustness test

4.3 Deceiving the classifier

It is possible to mislead the classifiers with false images. Fig. 7a shows an image obtained from Wikimedia that is classified as bread by its RGB features. Fig. 7b shows an image generated by a particle system Baravalle et al. (2011) which is classified as bread by its fractal and multifractal features. It is easy to deceive the RGB classifier, using images with similar color features as breads, but it is not clear how to do that with fractal features. We conclude that the fractal classifier is more accurate to discriminate these false images.

5 CONCLUSIONS AND FUTURE WORK

The utilisation of fractal and multifractal features in bread crumb texture classification showed good performance. The multifractal spectrum demonstrated to be accurate enough

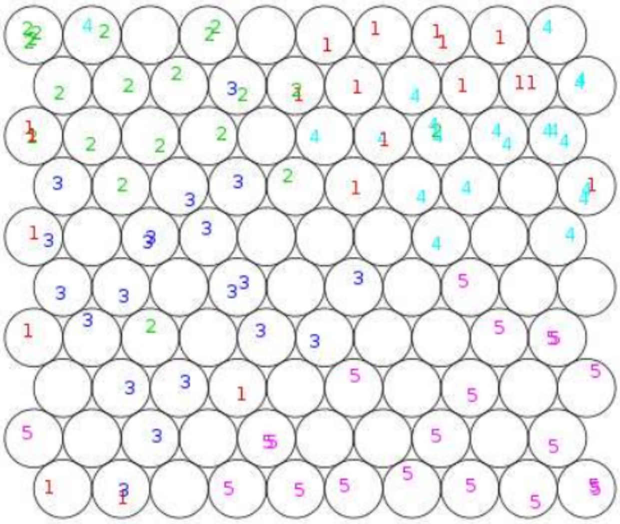

(a) Fractal features SOM

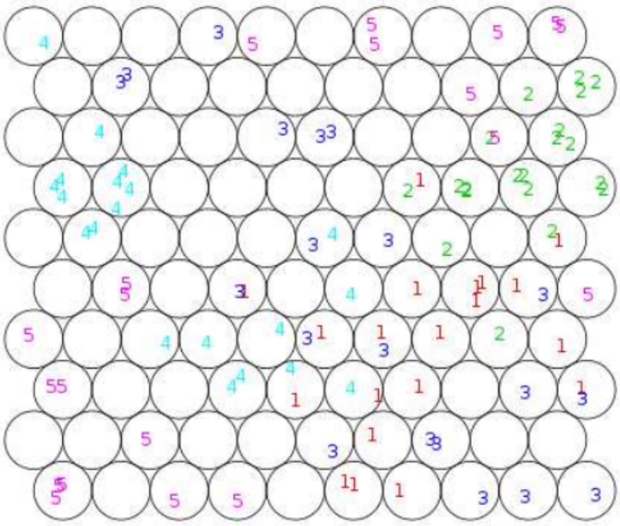

(b) SOM using RGB features

Figure 6: SOM of the scanned bread images (classes $1-4$) and the non bread images (class 5)

Classes	Baguette	Lactal	Salvado	Sandwich	Non bread
Baguette	0	9	0	11	0
Lactal	0	15	0	5	0
Salvado	0	6	0	12	2
Sandwich	0	10	0	10	0
Non bread	3	0	2	0	15

Table 3: Confusion Matrix for the fractal features

Classes	Baguette	Lactal	Salvado	Sandwich	Non bread
Baguette	0	0	0	0	20
Lactal	0	0	0	0	20
Salvado	0	0	0	0	20
Sandwich	0	0	0	0	20
Non bread	0	0	0	0	20

Table 4: Confusion Matrix for the RGB features

to perform a classification of differents bread types and also to discriminate non bread from bread images. The utilisation of non-fractal features such as color, also showed comparable results, but it fails to detect non bread images, and it is easy to deceive it with false images. Both methods showed to be sensitive to illumination changes, making the methods still non robust. Preliminary tests on our particle system Baravalle et al. (2011) show that it could deceive the fractal classifier, so further analysis is required in order to find the parameters that produce textures with similar fractal and multifractal features to those of real breads.

The results found can be applied to validate synthetic samples, i.e., the latter should have similar features to certain bread type that it is trying to simulate. The features obtained will be used to determine particle system parameters (e.g., lifetime of particles, color). These results can be extended to be used as quality parameters for these products. The robustness of the method needs to be enhanced. Other FDs will be studied in order to accomplish this goal. Also, the code of the multifractal spectrum algorithm is unoptimized, so optimisations needs to be applied in order to obtain a fast algorithm for bread classification. It will be useful to apply a Principal Component Analysis in order to identify the key variables in the feature vectors.

6 ACKNOWLEDGEMENTS

We would like to thank Gustavo Grieco and Pablo Speciale for technical discussions and for their support in the development of the present work.

REFERENCES

Andjelkovic J., Zivic N., Reljin B., Celebic V., and Salom I. Classifications of digital medical images with multifractal analysis. In *Proceedings of the 8th conference on Signal, Speech and image processing*, SSIP'08, pages 88–92. World Scientific and Engineering Academy and Society (WSEAS), Stevens Point, Wisconsin, USA, 2008. ISBN 978-960-6474-008-6.

Baravalle R., Delrieux C., and Gómez J.C. Síntesis de texturas utilizando sistemas de partículas. ECImag 2011. Actas de la Tercera Escuela y Workshop Argentino en Ciencias de las Imágenes. 2011.

(a) RGB features

(b) Mutilfractal features

Figure 7: Non bread images classified as bread by the evaluated classifiers

Baravalle R., Delrieux C., and Gómez J.C. Síntesis procedimental de materiales: resultados en el modelado de pan y materiales cocidos. Actas del XIV Workshop de Investigadores en Ciencias de la Computación (WICC), pages 21 – 26. 2012.

Boser B.E., Guyon I.M., and Vapnik V.N. A training algorithm for optimal margin classifiers. In *Proceedings of the fifth annual workshop on Computational learning theory*, COLT '92, pages 144–152. ACM, New York, NY, USA, 1992. ISBN 0-89791-497-X.

Chang C.C. and Lin C.J. LIBSVM: A library for support vector machines. *ACM Transactions on Intelligent Systems and Technology*, 2:27:1–27:27, 2011.

Fan Y. and Zhang H. Application of gabor filter and multi-class svm in baking bread quality classification. In *Mechatronics and Automation, Proceedings of the 2006 IEEE International Conference on*, pages 1498 –1502. 2006. doi:10.1109/ICMA.2006.257396.

Fei-Fei L., Fergus R., and Perona P. Learning generative visual models from few training examples an incremental bayesian approach tested on 101 object categories. In *Proceedings of the Workshop on Generative-Model Based Vision*. Washington, DC, 2004.

Gonzales-Barron U. and Butler F. Fractal texture analysis of bread crumb digital images. *European Food Research and Technology*, 226:721–729, 2008. ISSN 1438-2377. 10.1007/s00217-007-0582-3.

Huang L.K. and Wang M.J.J. Image thresholding by minimizing the measures of fuzziness. *Pattern Recognition*, 28(1):41 – 51, 1995. ISSN 0031-3203.

Imre A.R., Cseh D., Neteler M., and Rocchini D. Korcak dimension as a novel indicator of landscape fragmentation and re-forestation. *Ecological Indicators*, 11(5):1134–1138, 2011. ISSN 1470160X.

Kohonen T., Schroeder M.R., and Huang T.S., editors. *Self-Organizing Maps*. Springer-Verlag New York, Inc., Secaucus, NJ, USA, 3rd edition, 2001. ISBN 3540679219.

Mandelbrot B.B. Multifractal measures, especially for the geophysicist. *Pure and Applied Geophysics*, 131:5–42, 1989.

Otsu N. A Threshold Selection Method from Gray-level Histograms. *IEEE Transactions on Systems, Man and Cybernetics*, 9(1):62–66, 1979.

Peitgen H.O., Jürgens H., and Saupe D. Chaos and fractals: new frontiers of science. 2004.

Silvetti A. and Delrieux C. Multifractal analysis of medical images. Actas de la trigésimo novena Jornada Argentina de Informática e Investigación Operativa (JAIIO), pages 1575 –

1581. 2010.

Wendt H., Abry P., Jaffard S., Ji H., and Shen Z. Wavelet leader multifractal analysis for texture classification. In *Image Processing (ICIP), 2009 16th IEEE International Conference on*, pages 3829 –3832. 2009. ISSN 1522-4880.

White J.M. and Rohrer G.D. Image thresholding for optical character recognition and other applications requiring character image extraction. *IBM J. Res. Dev.*, 27(4):400–411, 1983. ISSN 0018-8646.

Yu L. and Qi D. Holder exponent and multifractal spectrum analysis in the pathological changes recognition of medical ct image. In *Control and Decision Conference (CCDC), 2011 Chinese*, pages 2040 –2045. 2011.